TUM-HEP-588/05

Prospects of the Coming Reactor and Accelerator Neutrino Experiments

Manfred Lindner
Physik Department, Technische Universität München
D-85748 Garching bei München, Germany
E-mail: lindner@ph.tum.de

ABSTRACT

Future reactor and long baseline neutrino oscillation experiments will lead to precision measurements of neutrino mass splittings and mixings. The flavour structure of the lepton sector will therefore at some point become better known than that of the quark sector. The potential of future oscillation experiments is discussed on the basis of detailed simulations with an emphasis on experiments which can be done in about ten years. In addition, some theoretical implications for neutrino mass models will be briefly discussed.

1. Introduction

The observation of atmospheric neutrino oscillations by the SuperKamiokande experiment[1)] triggered a remarkable discovery phase. The initial evidence turned into a solid proof of neutrino flavour conversions as well as of the L/E dependence as required by oscillations. The solar neutrino problem has also been resolved in the last years. The Gallex experiment[2)] detected initially a rate effect which implied flavour conversion on the basis of solar models. The SNO experiment proved then model independent neutrino flavour transitions[3,4)]. The initially allowed parameter islands were cleaned up by the KamLAND experiment, which demonstrated finally with reactor anti-neutrinos[5,6)] that the so-called LMA-solution is correct. Altogether the existing experimental results fit now very nicely into a picture with three massive neutrinos, which corresponds to the simplest scenario for three generations. The only exemption is the disputed LSND result[7)], which would have far reaching consequences if it were confirmed, but this possibility will be ignored here. The oscillations of three neutrino generations involve then two mass-squared differences $\Delta m^2_{12} \simeq \Delta m^2_{sol.}$ and $\Delta m^2_{23} \simeq \Delta m^2_{atm.}$, three mixing angles, θ_{12}, θ_{23}, and θ_{13}, and a CP-violating phase δ. Atmospheric neutrino data[8)] and the first results from the K2K long-baseline accelerator experiment[8)] determine $\Delta m^2_{23} = (2.2^{+0.6}_{-0.4}) \times 10^{-3}$ eV^2 and $\theta_{23} \approx 45^\circ$ [8,9)], whereas solar neutrino data[10,11)], combined with the results from the KamLAND reactor experiment[5)] lead to $\Delta m^2_{12} = (8.2^{+0.3}_{-0.3}) \times 10^{-5}$ eV^2 and $\tan^2\theta_{12} = 0.39^{+0.059}_{-0.04}$[9)]. The results can now approximatively be summarized by two independent two flavour oscillations where the solar and atmospheric Δm^2 values are roughly now known.

The key parameter for genuine three flavour effects is the mixing angle θ_{13} which is so far only known to be small from the CHOOZ[12,13)] and Palo Verde[14)] experiments. The current bound for θ_{13} depends on the value of the atmospheric mass squared

difference and it gets rather weak for $\Delta m^2_{31} \lesssim 2 \times 10^{-3}$ eV^2. However, in that region an additional constraint on θ_{13} from global solar neutrino data becomes important[15]. At the current best fit value of $\Delta m^2_{31} = 2.2 \times 10^{-3}$ eV^2 we have at 3σ the bound $\sin^2\theta_{13} \leq 0.041$[9]. There is no reason why θ_{13} should vanish and one should expect therefore θ_{13} to be finite.

Neutrino oscillations may appear less interesting in the future, since it might lead only to parameter improvements of the leading 2×2 oscillations and maybe a finite parameter value of θ_{13}. However, this misses completely the fact, that neutrinos may again uncover completely unexpected results, like sterile neutrinos or non-standard interactions. But there exists a very interesting physics program even if a standard three neutrino picture is correct. The point is that the neutrino sector is, unlike the quark sector, not obscured by (experimental and theoretical) hadronic uncertainties. The precision to which the underlying flavour information is determined will therefore only be limited by the ultimate experimental precision. If high precision measurements are possible, then they will be very sensitive tests of flavour models and related topics, like the unitarity of three flavours. Genuine three flavour oscillation effects occur only for a finite value of θ_{13} and establishing a finite value of θ_{13} is therefore one of the next milestones in neutrino physics. Leptonic CP violation is another three flavour effect which can only be tested if θ_{13} is finite. The usual see-saw scenario includes besides δ in addition two further Majorana CP phases in the light neutrino sector, as well as other CP phases in the heavy Majorana sector, which are involved in leptogenesis. In general the heavy and light CP phases are not connected, but most flavour models create relations between these two sectors, relating thus low energy leptonic CP violation to leptogenesis and mass models. Precision measurements of neutrino oscillations test therefore very interesting questions of particle physics which are connected to the origin of flavour and to phenomenological consequences of flavour. There is thus a very strong motivation to establish first in the next generation of experiments a finite value of θ_{13} in order to aim in the long run at a measurement of leptonic CP violation[16,17,18,19,20].

2. Three neutrino oscillation in matter

Future precision oscillation experiments require a full three flavour formalism and the inclusion of matter effects. Generalization of the two flavour oscillation formulae in vacuum to the vacuum probabilities for flavour transitions $\nu_{f_l} \to \nu_{f_m}$ of N neutrinos leads to

$$P(\nu_{f_l} \to \nu_{f_m}) = \underbrace{\delta_{lm} - 4 \sum_{i>j} \mathrm{Re} J^{f_l f_m}_{ij} \sin^2 \Delta_{ij}}_{P_{CP}} \underbrace{-2 \sum_{i>j} \mathrm{Im} J^{f_l f_m}_{ij} \sin 2\Delta_{ij}}_{P_{\not{CP}}} \qquad (1)$$

where the shorthands $J^{f_l f_m}_{ij} := U_{li} U^*_{lj} U^*_{mi} U_{mj}$ and $\Delta_{ij} := \frac{\Delta m^2_{ij} L}{4E}$ have been used. These

generalized vacuum transition probabilities depend on all combinations of quadratic mass differences $\Delta m^2_{ij} = m^2_i - m^2_j$ as well as on different products of elements of the leptonic mixing matrix U. We will assume a three neutrino framework, i.e. $1 \leq i, j \leq 3$ and U is a 3×3 mixing matrix parameterized in the standard way

$$U = \begin{pmatrix} c_{12}c_{13} & s_{12}c_{13} & s_{13}e^{-i\delta} \\ -s_{12}c_{23} - c_{12}s_{23}s_{13}e^{i\delta} & c_{12}c_{23} - s_{12}s_{23}s_{13}e^{i\delta} & s_{23}c_{13} \\ s_{12}s_{23} - c_{12}c_{23}s_{13}e^{i\delta} & -c_{12}s_{23} - s_{12}c_{23}s_{13}e^{i\delta} & c_{23}c_{13} \end{pmatrix} , \qquad (2)$$

where $c_{ij} = \cos(\theta_{ij})$ and $s_{ij} = \sin(\theta_{ij})$. U contains three leptonic mixing angles and one Dirac-like leptonic CP phase δ. Note that the most general mixing matrix for three Majorana neutrinos contains two further Majorana-like CP phases, but it can easily be seen that these extra phases do not enter in the above oscillation formulae. Disappearance probabilities, *i.e.* the transitions $\nu_{f_l} \to \nu_{f_l}$, do not even depend on δ, since $J^{f_l f_l}_{ij}$ is only a function of the modulus of elements of U. Appearance probabilities, like $\nu_e \to \nu_\mu$ are therefore the place where leptonic CP violation can be studied. Eq. (1) contains a CP conserving part P_{CP} and a CP violating part $P_{\not CP}$, and both terms depend on the CP phase δ. An obvious extraction strategy for CP-violation would thus be to look at CP asymmetries[21]. Note, however, that the beams of a long baseline experiment traverse the Earth and the presence of matter violates CP by itself. This implies modifications of eq. (1) and it makes a measurement of leptonic CP violation more involved.

Eq. (1) leads to well known, but somewhat lengthy vacuum oscillation formulae which many trigonometric terms. These expressions become even longer, and do not exist in closed form, when arbitrary matter corrections are taken into account. For effectively constant matter densities, which is often a good assumption, the problem simplifies somewhat, but the general oscillation probabilities are still quite complex expressions. The Hamiltonian which describes three neutrino oscillation in matter can then be written in flavour basis as

$$H = \frac{1}{2E_\nu} U \begin{pmatrix} m^2_1 & 0 & 0 \\ 0 & m^2_2 & 0 \\ 0 & 0 & m^2_3 \end{pmatrix} U^T + \frac{1}{2E_\nu} \begin{pmatrix} A + A' & 0 & 0 \\ 0 & A' & 0 \\ 0 & 0 & A' \end{pmatrix} . \qquad (3)$$

The first term describes oscillations in vacuum in flavour basis. The quantities A and A' in the second term are given by the charged current and neutral current contributions to coherent forward scattering in matter. The charged current contribution is given by

$$A = \pm \frac{2\sqrt{2} G_F Y \rho E_\nu}{m_n} = 2VE_\nu , \qquad (4)$$

where G_F is Fermi's constant, Y is the number of electrons per nucleon, m_n is the nucleon mass and ρ is the matter density. A is positive for neutrinos in matter and anti-neutrinos in anti-matter, while it is negative for anti-neutrinos in matter and

neutrinos in anti-matter. The flavour universal neutral current contributions A' lead to an overall phase which does not enter the transition probabilities. The over-all neutrino mass scale m_1^2 can be written as a term proportional to the unit matrix and can similarly be removed, such that only Δm^2_{21} and Δm^2_{31} remain in the first term of eq. (3). After re-diagonalization of the Hamiltonian in constant matter density one finds that matter effects lead in a very good approximation to an A-dependent parameter mapping in the 1-3 subspace which can be written as[22)]

$$\sin^2 2\theta_{13,m} = \frac{\sin^2 2\theta_{13}}{C_\pm^2} , \tag{5}$$

$$\Delta m^2_{31,m} = \Delta m^2_{31} C_\pm , \tag{6}$$

$$\Delta m^2_{32,m} = \frac{\Delta m^2_{31}\ (C_\pm + 1) + A}{2} , \tag{7}$$

$$\Delta m^2_{21,m} = \frac{\Delta m^2_{31}\ (C_\pm - 1) - A}{2} . \tag{8}$$

The index m denotes effective quantities in matter, where

$$C_\pm^2 = \left(\frac{A}{\Delta m^2_{31}} - \cos 2\theta \right)^2 + \sin^2 2\theta . \tag{9}$$

Note that A in $C_\pm$ can change its sign and the mappings for neutrinos and anti-neutrinos are therefore different, resulting in different effective mixings and masses. This is an important effect, which will allow detailed tests of coherent forward scattering of neutrinos in matter. Note that oscillations in matter depend unlike vacuum oscillations on the sign of Δm^2_{31}. This allows to extract the $sign(\Delta m^2_{31})$ via matter effects.

Inserting the parameter mappings eqs. (5)-(8) into the full oscillation formulae leads still to quite lengthy expressions for the oscillation probabilities in matter, where it is not easy to oversee all effects. It is therefore instructive to simplify the problem further such that a qualitative analytic understanding of all effects becomes possible, while quantitative statements should be evaluated numerically with the full expressions. The key for further simplification is to expand the oscillation probabilities in small quantities. These expansion parameters are $\alpha = \Delta m^2_{21}/\Delta m^2_{31}$ =O(10^{-2}) and $\sin^2 2\theta_{13} \leq 0.16$. The matter effects can be parameterized by the dimensionless quantity $\hat{A} = A/\Delta m^2_{31} = 2VE/\Delta m^2_{31}$, where $V = \sqrt{2} G_F n_e$. The oscillation probabilities for all channels can in this way be significantly simplified[23)]. Using $\Delta \equiv \Delta_{31}$, the

leading terms for $P(\nu_\mu \to \nu_\mu)$ and $P(\nu_e \to \nu_\mu)$ can, for example, be written as[17,24,22)]

$$P(\nu_\mu \to \nu_\mu) \approx$$
$$1 - \cos^2\theta_{13}\sin^2 2\theta_{23}\sin^2\Delta + 2\ \alpha\ \cos^2\theta_{13}\cos^2\theta_{12}\sin^2 2\theta_{23}\Delta\cos\Delta, \qquad (10)$$

$$P(\nu_e \to \nu_\mu) \approx \sin^2 2\theta_{13}\sin^2\theta_{23}\ \ \frac{\sin^2((1-\hat{A})\Delta)}{(1-\hat{A})^2}$$
$$\pm \sin\delta\cdot\sin 2\theta_{13}\ \alpha\ \sin 2\theta_{12}\cos\theta_{13}\sin 2\theta_{23}\sin(\Delta)\frac{\sin(\hat{A}\Delta)\sin((1-\hat{A})\Delta)}{\hat{A}(1-\hat{A})}$$
$$+ \cos\delta\cdot\sin 2\theta_{13}\ \alpha\ \sin 2\theta_{12}\cos\theta_{13}\sin 2\theta_{23}\cos(\Delta)\frac{\sin(\hat{A}\Delta)\sin((1-\hat{A})\Delta)}{\hat{A}(1-\hat{A})}$$
$$+\ \alpha^2\ \sin^2 2\theta_{12}\cos^2\theta_{23}\frac{\sin^2(\hat{A}\Delta)}{\hat{A}^2}\ , \qquad (11)$$

where "+" in eq. (11) stands for neutrinos and "−" for anti-neutrinos. The most important feature of eq. (11) is that all interesting effects in the $\nu_e \to \nu_\mu$ transition depend crucially on θ_{13}. The size of $\sin^2 2\theta_{13}$ determines thus if the total transition rate, matter effects, effects due to the sign of Δm^2_{31} and CP violating effects are measurable. This is the reason why the size of θ_{13} is one of the most important questions for future oscillation experiments.

Before we discuss some features of eqs. (10) and (11) in more detail, we would like to comment on the underlying assumptions and the reliability of these equations. First eqs. (10) and (11) are an expansion in terms of the small quantities α and $\sin 2\theta_{13}$. Higher order terms are suppressed at least by another power of one of these small parameters and these corrections are thus typically at the percent level. Note that the expansion in α is actually an expansion in the solar and not the atmospheric frequency. The expansion does therefore not break down at the first atmospheric oscillation maximum, i.e. at $\Delta \simeq 1$, but at much larger baselines before the first (sub-dominant) solar oscillation maximum, i.e. at $\alpha\Delta \simeq 1$. The latter condition gives an upper bound for the baseline where eqs. (10) and (11) are good approximations

$$L \lesssim 8000\,\mathrm{km}\left(\frac{E_\nu}{GeV}\right)\left(\frac{10^{-4}\mathrm{eV}^2}{\Delta m^2_{21}}\right)\ , \qquad (12)$$

while the first oscillation maximum sits at $\alpha\cdot L \simeq L/30$. Eqs. (10) and (11) are therefore excellent approximations at and well beyond the first oscillation maximum of long baseline experiments. The matter corrections in eqs. (10) and (11) are derived for constant average matter density which is a good approximation.

Note that all quantitative results which will be presented are based on numerical simulations in matter. The results are therefore not affected by any approximation. Eqs. (10) and (11) will only be used to understand the problem analytically, which is extremely helpful in order to oversee the multi-dimensional parameter space.

In addition to long baseline experiments, reactor experiments with identical near and far detectors have an excellent potential for precise measurements. The near detector is used to eliminate many common systematical errors and the far detector is located typically at a baseline of a few kilometer. For these short baselines matter effects can be ignored and one finds to second order in the small quantities $\sin 2\theta_{13}$ and α for the oscillation probability

$$1 - P_{\bar{e}\bar{e}} = \sin^2 2\theta_{13} \, \sin^2 \Delta_{31} + \alpha^2 \, \Delta_{31}^2 \, \cos^4 \theta_{13} \, \sin^2 2\theta_{12} \, . \tag{13}$$

At the first atmospheric oscillation maximum, Δ_{31} is approximately $\pi/2$ and $\sin^2 \Delta_{31}$ is close to one, which means that the second term on the right-hand side of this equation can be neglected for $\sin^2 2\theta_{13} \gtrsim 10^{-3}$. The reactor measurement is dominated in this case at short baselines by the product of $\sin^2 2\theta_{13}$ and $\sin^2 \Delta_{31}$, which must be measured as deviation from one. Eq. (13) implies that correlations and degeneracies play essentially no role in reactor experiments. The behavior in the $\sin^2 2\theta_{13}$-Δm^2_{21}-plane will also be different since eq. (13) is essentially independent of Δm^2_{21}. A reactor experiment will improve the global parameter determination in two ways. First, a direct, essentially uncorrelated and clean measurement for θ_{13}[25)] can be obtained which can be used to disentangle the long baseline results. Secondly, the reactor measurement can replace the cross-section suppressed anti-neutrino running of the accelerator experiments, leading to statistical improvements in the neutrino measurements[26)].

3. Correlations and degeneracies

Eqs. (10) and (11) exhibit certain parameter correlations and degeneracies, which play an important role in the analysis of long baseline experiments, and which would be hard to understand in a purely numerical analysis of the high dimensional parameter space. The most important properties are:

- Eqs. (10) and (11) depend only on the product $\alpha \cdot \sin 2\theta_{12}$ or equivalently $\Delta m^2_{21} \cdot \sin 2\theta_{12}$. This are the parameters related to solar oscillations which will be taken as external input. Note that the product is better determined than the product of the individual measurements of Δm^2_{21} and $\sin 2\theta_{12}$.

- Next we observe in eq. (11) that the second and third term contain both a factor $\sin(\hat{A}\Delta)$, while the last term contains a factor $\sin^2(\hat{A}\Delta)$. Since $\hat{A}\Delta = VL/2$, we find that these factors depend only on L, resulting in a "magic baseline" [27)] when $VL_{magic} = 2\pi$, where $\sin(\hat{A}\Delta)$ vanishes. At this magic baseline only the first term in eq. (11) survives and $P(\nu_e \to \nu_\mu)$ does no longer depend on δ, α and $\sin 2\theta_{12}$. This is in principle very important, since it implies that $\sin^2 2\theta_{13}$ can be determined at the magic baseline from the first term of eq. (11) whatever the values and errors of δ, α and $\sin 2\theta_{12}$ are. For the given matter density of the Earth we find $L_{magic} = 2\pi/V \simeq 8100$ km which fits nicely into the Earth.

This value is quite amazing, since V is given in terms of completely unrelated constants of nature like G_F.

- Next we observe that only the second and third term of eq. (11) depend on the CP phase δ, and both terms contain a factor $\sin 2\theta_{13} \cdot \alpha$, while the first and fourth term of eq. (11) do not depend on the CP phase δ and contain factors of $\sin^2 2\theta_{13}$ and α^2, respectively. The extraction of CP violation is thus always suppressed by the product $\sin 2\theta_{13} \cdot \alpha$ and the CP violating terms are obscured by large CP independent terms if either $\sin^2 2\theta_{13} \ll \alpha^2$ or $\sin^2 2\theta_{13} \gg \alpha^2$. The relative contribution of the CP phase δ to the probability is thus largest for $\sin^2 2\theta_{13} \simeq 4\theta_{13}^2 \simeq \alpha^2$.

- Another observation is that the last term in eq. (11), which is proportional to $\alpha^2 = (\Delta m^2_{21})^2/(\Delta m^2_{31})^2$, dominates in the limit of tiny $\sin^2 2\theta_{13}$. The error of Δm^2_{21} limits therefore for small $\sin^2 2\theta_{13}$ the parameter extraction. This last term implies a finite transition probability even for $\theta_{13} = 0$. Observing $\nu_e \to \nu_\mu$ or $\nu_\mu \to \nu_e$ appearance transitions does therefore not necessarily establish a finite value of $\theta_{13} = 0$ in a three flavour framework.

- Eqs. (10) and (11) suggest that transformations exist which leave these equations invariant. Therefore degeneracies, *i.e.* parameter sets having identical oscillation probabilities for a fixed L/E are expected. An example of such an invariance is given by a simultaneous replacement of neutrinos by anti-neutrinos and $\Delta m^2_{31} \to -\Delta m^2_{31}$. This is equivalent to changing the sign of the second term of eq. (11) and replacing $\alpha \to -\alpha$ and $\Delta \to -\Delta$, while $\hat{A} \to \hat{A}$. It is easy to see that eqs. (10) and (11) are unchanged, but this is not a degeneracy, since neutrinos and anti-neutrinos can be distinguished experimentally.

- The first real degeneracy[28,29] can be seen in the disappearance probability eq. (10), which is invariant under the replacement $\theta_{23} \to \pi/2 - \theta_{23}$. Note that the second and third term in eq. (11) are not really invariant under this transformation, but this change in the sub-leading appearance probability can approximately be compensated by tiny parameter shifts. This implies that the degeneracy can in principle be lifted with high precision measurements in the disappearance channels.

- The second degeneracy can be found in the appearance probability eq. (11) in the $(\delta - \theta_{13})$-plane[30,31]. In terms of θ_{13} (which is small) and δ the four terms of eq. (11) have the structure

$$P(\nu_e \to \nu_\mu) \approx \theta_{13}^2 \cdot F_1 + \theta_{13} \cdot (\pm \sin\delta F_2 + \cos\delta F_3) + F_4 \ , \qquad (14)$$

where the quantities F_i, $i = 1, .., 4$ contain all the other parameters. The requirement $P(\nu_e \to \nu_\mu) = const.$ leads for both neutrinos and anti-neutrinos

to parameter manifolds of degenerate or correlated solutions. Having both neutrino and anti-neutrino beams, the two channels can be used independently, which is equivalent to considering simultaneously eq. (14) for $F_2 \equiv 0$ and $F_3 \equiv 0$. The requirement that these probabilities are now independently constant, *i.e.* $P(\nu_e \to \nu_\mu) = const.$ for $F_2 \equiv 0$ and $F_3 \equiv 0$, leads to more constraint manifolds in the $(\delta - \theta_{13})$-plane, but some degeneracies still survive.

- The third degeneracy[32] is given by the fact that a change in sign of Δm^2_{31} can essentially be compensated by an offset in δ. Therefore we note again that the transformation $\Delta m^2_{31} \to -\Delta m^2_{31}$ leads to $\alpha \to -\alpha$, $\Delta \to -\Delta$ and $\hat{A} \to -\hat{A}$. All terms of the disappearance probability, eq. (10), are invariant under this transformation. The first and fourth term in the appearance probability eq. (10), which do not depend on the CP phase δ, are also invariant. The second and third term of eq. (10) depend on the CP phase and change by the transformation $\Delta m^2_{31} \to -\Delta m^2_{31}$. The fact that these changes can be compensated by an offset in the CP phase δ is the third degeneracy.

- Altogether there exists an eight-fold degeneracy [29], as long as only the $\nu_\mu \to \nu_\mu$, $\bar{\nu}_\mu \to \bar{\nu}_\mu$, $\nu_e \to \nu_\mu$ and $\bar{\nu}_e \to \bar{\nu}_\mu$ channels and one fixed L/E are considered. However, eqs. (10) and (11) also imply that the degeneracies can be broken by using in a suitable way information from different L/E values. This can be achieved in total event rates by changing or combining different L or E[33,34,35], but it can in principle also be done by using information in the event rate spectrum of a single baseline L, which requires detectors with very good energy resolution[17]. Another strategy to break the degeneracies is to include further oscillation channels in the analysis ("silver channels")[33,36].

The discussion of this section shows the strength of the analytic approximations, which allow to understand the complicated parameter interdependence. It also helps to optimally plan experimental setups and to find strategies to resolve the degeneracies.

4. The potential of future neutrino oscillation experiments

Building on the success of previous experiments, various plans for future projects are under discussion. Some projects are even under construction or have already been completed. It is interesting to explore where these experiments will bring us in the determination of neutrino oscillation parameters in about ten years from now. It is also interesting to look further into the future and to estimate the ultimate precision which could be obtained.

The precision of quantities like $\sin^2 2\theta_{13}$ which is found form the simulation of experiments will be presented in a way shown in fig. 1. The bands show how the initial value, which is given by statistics alone (left edge of blue/dark grey band) deteriorates

by systematic errors, by parameter correlations (e.g. with the unknown or partly known CP phase) and parameter degeneracies (due to trigonometric ambiguities). It is important to note that a given experiment (or combination of experiments) typically measures some parameter combination with a precision which is considerably better than the final limit. This precision of the experiment is shown in fig. 1 as the right edge of the blue/dark grey band. This precision might be called $\left(\sin^2 2\theta_{13}\right)_{eff}$, since it expresses the precision if all other unknown parameters are fixed and no errors are included. However, if one properly extracts a limit of $\sin^2 2\theta_{13}$ with all unknowns properly taken into account, then one ends up at the right edge of the yellow/light grey band. Distinguishing in this way between the precision and the sensitivity is quite useful, since it also shows the room for improvement by combinations with other similarly precise experiments with other parameter dependence.

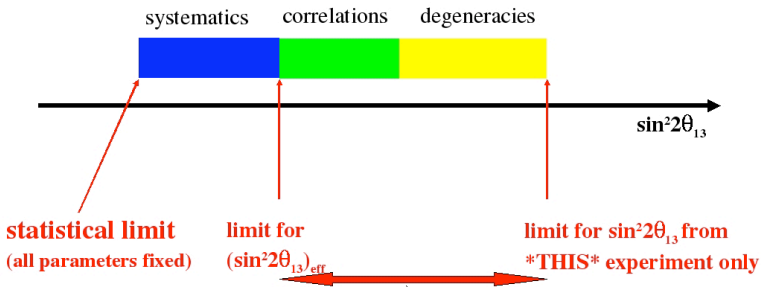

Figure 1: The precision for $\sin^2 2\theta_{13}$ is shown in colored bands, where the left edge of the blue/dark grey band shows the initial value which is obtained if only statistics is considered. The right edge of the blue/dark grey band is the result after the systematic errors are included. This is the principal precision of the experiment. However, the sensitivity for $\sin^2 2\theta_{13}$ deteriorates further due to parameter correlations and parameter degeneracies. The final value is the right edge of the yellow/light grey band. The range covered by the green and yellow bands can lead to remarkable synergies when this experiment is combined with another experiment with similar precision, but different parameter dependence.

4.1. Next generation experiments

Future oscillation experiments can be grouped according to their time scale of operation. The K2K experiment is already running and its results tests the leading atmospheric oscillation already now. The MINOS experiment has recently started and the CNGS projects is nearing the completion of construction. We include therefore in our study the conventional next generation beam experiments MINOS[37], as well as the CNGS experiments ICARUS[38] and OPERA[39]. We include also the subsequent superbeam experiments J-PARC to SuperKamiokande (T2K)[40] and NuMI off-axis (NOνA)[41], as well as new reactor neutrino experiments[42] with a near and far detector. The main characteristics of these experiments are summarized in tab. 1. For the reactor experiments we use the Double-Chooz proposal (D-CHOOZ)[43] as initial stage

setup with roughly 6×10^4 events, and an optimized setup called Reactor-II, with a slightly longer baseline and 6×10^5 events. Such a configuration could be realized at several other sites under discussion[42]. The results presented in the following are based on Ref.[44], where more details on the analysis can be found. The simulations of the experiments as well as the statistical analysis is performed with the GLoBES software package[45].

Label	L [km]	$\langle E_\nu \rangle$	$t_{\rm run}$	channel
Conventional beam experiments:				
MINOS	735	3 GeV	5 yr	$\nu_\mu \to \nu_{\mu,e}$
ICARUS	732	17 GeV	5 yr	$\nu_\mu \to \nu_{e,\mu,\tau}$
OPERA	732	17 GeV	5 yr	$\nu_\mu \to \nu_{e,\mu,\tau}$
Off-axis superbeams:				
T2K	295	0.76 GeV	5 yr	$\nu_\mu \to \nu_{e,\mu}$
NOνA	812	2.22 GeV	5 yr	$\nu_\mu \to \nu_{e,\mu}$
Reactor experiments:				
D-CHOOZ	1.05	~ 4 MeV	3 yr	$\nu_e \to \nu_e$
Reactor-II	1.70	~ 4 MeV	5 yr	$\nu_e \to \nu_e$

Table 1: Characteristics of the considered experiments.

A first interesting question concerns improvements of Δm^2_{31} and $\sin^2\theta_{23}$. In tab. 2 we show the precision which can be obtained in the future in comparison to the current precision, as obtained from a global fit to SuperKamiokande (SK) atmospheric and K2K long-baseline data[15]. The last row is the precision which can be obtained by combining all experiments. We observe from these numbers, that the accuracy on Δm^2_{31} can be improved by one order of magnitude, whereas the accuracy on $\sin^2\theta_{23}$ will be improved only by a factor two.

	$\lvert\Delta m^2_{13}\rvert$	$\sin^2\theta_{23}$
current	88%	79%
MINOS+CNGS	26%	78%
T2K	12%	46%
NOνA	25%	86%
Combination	9%	42%

Table 2: Precision for $|\Delta m^2_{31}|$ and $\sin^2\theta_{23}$ at 3σ for the values $\Delta m^2_{31} = 2 \times 10^{-3}$ eV^2, $\sin^2\theta_{23} = 0.5$.

Tab. 2 depends on the value of Δm^2_{31} which is shown in fig. 2. The sensitivity suffers for all experiments for low values of Δm^2_{31}. T2K will provide a precise determination of Δm^2_{31} at the level of a few percent for $\Delta m^2_{31} \gtrsim 2 \times 10^{-3}$ eV^2. Although NOνA can put a comparable lower bound on Δm^2_{31}, the upper bound is significantly weaker, and similar to the bound from MINOS. The reason for this is a strong correlation between Δm^2_{31} and θ_{23}, which disappears only for $\Delta m^2_{31} \gtrsim 3 \times 10^{-3}$ eV^2. From

the right panel of fig. 2 one can see that for $\Delta m^2_{31} \sim 2 \times 10^{-3}$ eV^2 only T2K is able to improve the current bound on $\sin^2 \theta_{23}$. One reason for the rather poor performance on $\sin^2 \theta_{23}$ is the fact that these experiments are sensitive mainly to $\sin^2 2\theta_{23}$. This implies that for $\theta_{23} \approx \pi/4$ it is very hard to achieve a good accuracy on $\sin^2 \theta_{23}$, although $\sin^2 2\theta_{23}$ can be measured with relatively high precision[46].

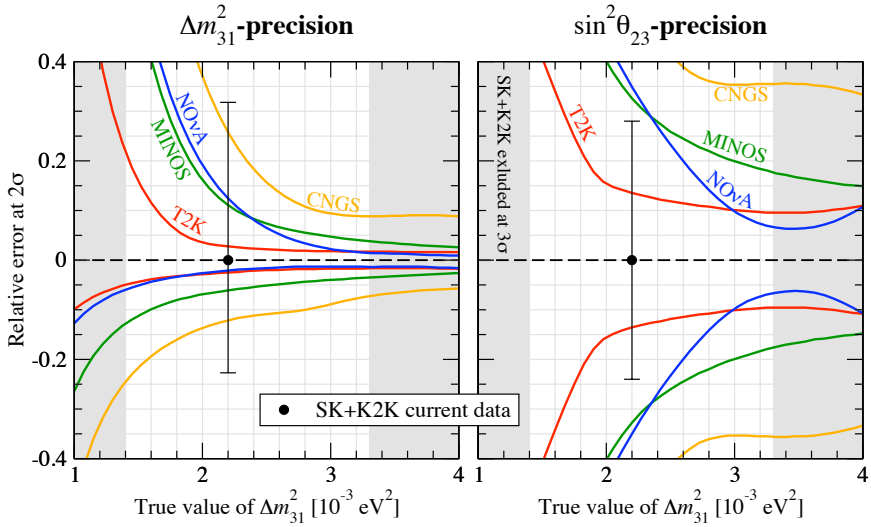

Figure 2: The precision of Δm^2_{31} (left panel) and $\sin^2 \theta_{23}$ (right panel) as a function of the "true value" of Δm^2_{31} for $\theta_{23}^{\rm true} = \pi/4$ (from Ref. [47]).

Another interesting question is if the next generation long baseline experiments which will operate in the next years will be able to test the three flavourness of the oscillations. The sensitivity to a finite value of the key parameter θ_{13} is shown in fig. 3 for MINOS, OPERA and ICARUS. It can be seen that these experiments have only a modest potential for improvements of the existing θ_{13} limit.

The combined sensitivity to $\sin^2 2\theta_{13}$ of the next-to-next generation experiments is compared in the left panel of fig. 4 with new reactor experiments, T2K (JPARC-SK) and NOνA (NuMI). It can be seen that the $\sin^2 2\theta_{13}$-limits from beam experiments are strongly affected by parameter correlations and degeneracies, whereas reactor experiments provide a "clean" measurement of $\sin^2 2\theta_{13}$, dominated by statistics and systematics[48].

The dependence of the $\sin^2 2\theta_{13}$-limit on the value of Δm^2_{31} is shown in the right panel of fig. 4, where the sensitivity of all experiments gets again rather poor for low values of Δm^2_{31}. For $\Delta m^2_{31} \sim 2 \times 10^{-3}$ eV^2 we find roughly an improvement by a factor 2 from conventional beam experiments (MINOS+ICARUS+OPERA combined), a factor 4 from Double Chooz (D-CHOOZ), and a factor 6 from the superbeams T2K and NOνA with respect to the current bound from global data[15]. Note that an optimized reactor experiment such as Reactor-II has the potential for even better

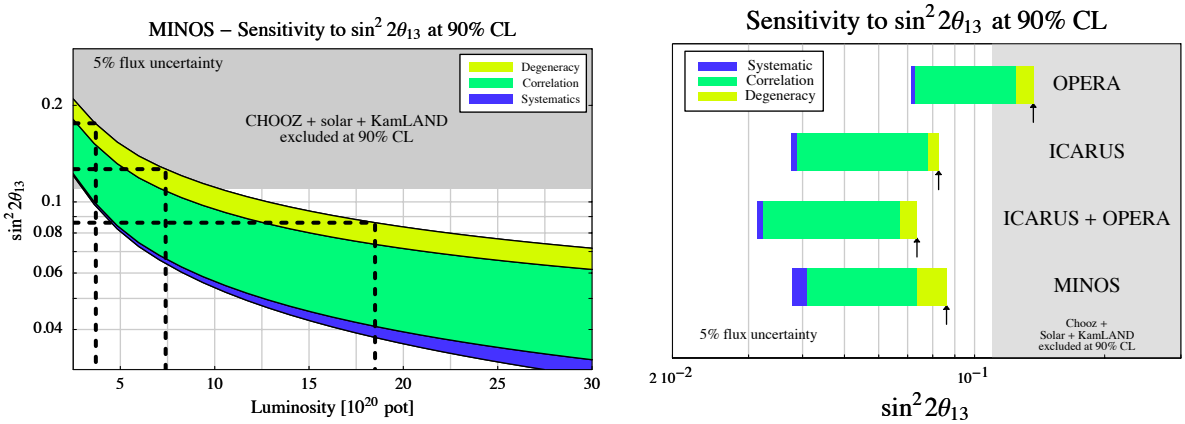

Figure 3: Left plot: The sensitivity of the MINOS experiment to θ_{13} as a function of the protons on target (pot) assuming a 5% flux uncertainty. The dashed lines represent what 1,2 and 5 years of operation might achieve (from left to right). Right plot: Comparison of 5 years of operation for the MINOS and CNGS experiments. The grey area for large $\sin^2 2\theta_{13}$ indicates in all cases the current limit from the CHOOZ experiment. The color code of the error bars is explained in fig. 1. Further details can be found in [44].

$\sin^2 2\theta_{13}$-sensitivities than the superbeams (c.f. left panel of fig. 4).

4.2. Synergies

The previous discussion shows that complimentary and partly competing plans with similar potential might be realized at the same time scale. This allows to combine the statistics of similar experiments leading to improved global fits. However, it is also possible to utilize synergies between experiments which are more than the simple combination of statistics. One aspect is here the fact that individual experiments measure some parameter combinations with certain degeneracies and correlations. Experiments with similar sensitivities, but with different correlations and degeneracies allow to separate the parameters partly or almost fully. An example of such a discussion is given by combining the T2K and NOνA experiments for a fixed time of operation in the best possible way. T2K is essentially insensitive to matter effects, while matter effects play already some role for the longer NOνA baselines. Both experiments could run partly with neutrino and partly with anti-neutrino beams. A second synergy aspect lies in the cross-sections for anti-neutrinos, which are smaller than neutrino cross-sections, leading to fewer events for the same running period. An anti-neutrino running is moreover in many aspects like a different experiment, but it is clear that anti-neutrino information is crucial in order to resolve the parameters. A comparable reactor neutrino experiment would lead to two kinds of synergy, since it could provide the required anti-neutrino information and it would allow in addition T2K and NOνA to run (at least initially) fully in neutrino mode, with more events

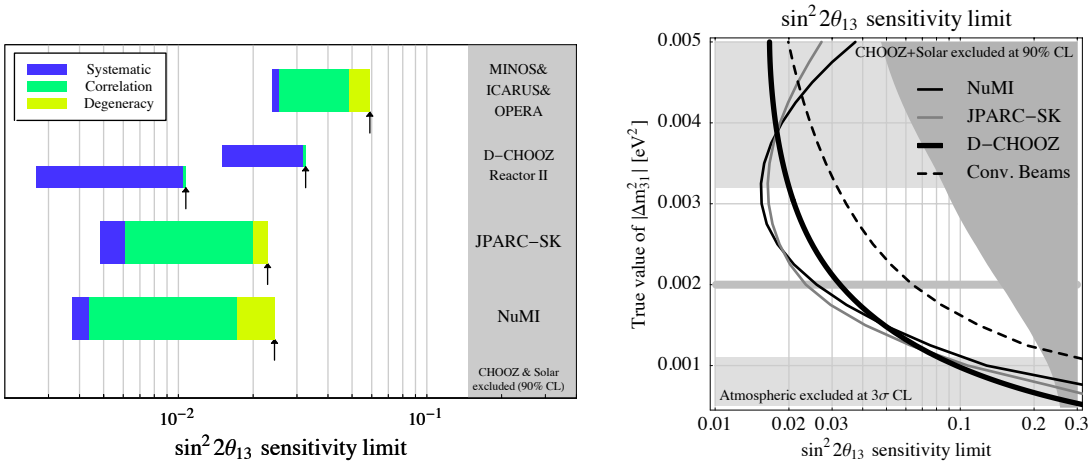

Figure 4: Left plot: Sensitivity to $\sin^2 2\theta_{13}$ at 90% CL for $\Delta m^2_{31} = 2 \times 10^{-3}$ eV^2, $\Delta m^2_{21} = 7 \times 10^{-5}$ eV^2. Right plot: Sensitivity to $\sin^2 2\theta_{13}$ at 90% CL as a function of the "true value" of Δm^2_{31}.

and therefore better statistics.

Such a synergetic combination would be especially interesting if $\sin^2 2\theta_{13}$ would be close to the current bound. In order to demonstrate these synergy effects we assume that $\sin^2 2\theta_{13} = 0.1$ and investigate what we could be learned about the CP-phase δ and the neutrino mass ordering. First we note that T2K, NOνA and the reactor experiment will all be able to establish the non-zero value of $\sin^2 2\theta_{13}$. However, depending on the unknown value of δ different values of $\sin^2 2\theta_{13}$ will be allowed. This can be seen as allowed regions in the θ_{13}-δ-plane shown in Figs. 8 and 9 of Ref.[44]. None of the experiments on their own can give any information on the CP-phase δ and on the mass hierarchy. The determination of $\sin^2 2\theta_{13}$ from beam experiments is strongly affected by the correlations with δ, and especially for NOνA also correlations with other parameters are important. Moreover, the inability to rule out the wrong mass hierarchy leads to a further ambiguity in the determination of $\sin^2 2\theta_{13}$. In contrast, since the $\bar{\nu}_e$-survival probability does not depend on δ, Reactor-II provides a clean determination of $\sin^2 2\theta_{13}$ at the level of 20% at 90% CL. If all experiments are combined the complementarity of reactor and beam experiments allows to exclude up to 40% of all possible values of the CP-phase for a given hierarchy. The wrong hierarchy can be ruled out at a modest confidence level with $\Delta\chi^2 \simeq 3$ due to matter effects in NOνA. However, at high confidence levels all values of δ are allowed, and moreover, even for a given hierarchy CP-conserving and CP-violating values of δ cannot be distinguished at 90% CL. These results depend also to some extent on the value of δ.

So far we have considered only neutrino running for the superbeams, since it is unlikely that significant data can be collected with anti-neutrinos within ten years from now. Nevertheless, it is interesting to investigate the potential of a neutrino-anti-neutrino comparison. In fig. 5 we show the results from T2K+NOνA with 3

years of neutrinos plus 3 years of anti-neutrinos each (left), in comparison with the case where the anti-neutrino running is replaced by Reactor-II (right). We find that anti-neutrino data at that level does neither solve the problems related to the CP-phase nor to the hierarchy. Still CP-violating and CP-conserving values cannot be distinguished at 90% CL. Moreover, the determination of $\sin^2 2\theta_{13}$ is less precise than from the reactor measurement. To benefit from anti-neutrino measurements a significantly longer measurement period would be necessary, to obtain large enough data samples. Given the fact that a reactor experiment is considerably cheaper than the beam experiments, it would probably be better to compare 3+3 years beams without a reactor experiment with 6 years of neutrino running of the beams plus a reactor. The reactor experiment would provide a precise $\sin^2 2\theta_{13}$ measurement and the beam experiments would collect more statistics by fully running in neutrino mode.

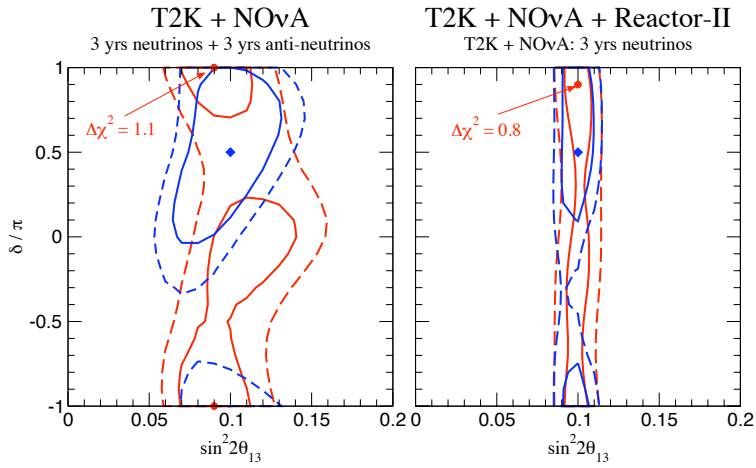

Figure 5: Anti-neutrino running vs Reactor-II. We show the 90% CL (solid curves) and 3σ (dashed curves) allowed regions in the $\sin^2 2\theta_{13}$-δ-plane for the assumed values $\sin^2 2\theta_{13} = 0.1$ and $\delta = \pi/2$. The blue/dark curves refer to the allowed regions for the normal mass hierarchy, whereas the red/light curves refer to the $\mathrm{sgn}(\Delta m^2_{31})$-degenerate solution (inverted hierarchy), where the projections of the minima onto the $\sin^2 2\theta_{13}$-δ-plane are shown as diamonds (normal hierarchy) and dots (inverted hierarchy). For the latter, the $\Delta\chi^2$-value with respect to the best-fit point is also given.

4.3. Long term perspectives

Beyond the discussed accelerator and reactor based oscillation experiments there exist more ambitious projects like the JHF-HyperKamiokande project, beta beams and neutrino factories. Such experiments clearly require further R&D both on the accelerator as well as on the detector side before they can be built. However, assuming current knowledge, we are quite certain that such setups are possible in the future. In order to demonstrate the power of such setups we show the potential of the JHF-HyperKamiokande experiment and a neutrino factory in fig. 6 in comparison to T2K (JHF-SK) and NOνA. It can be seen that the existing limits can be improved by a

few orders of magnitude compared to now.

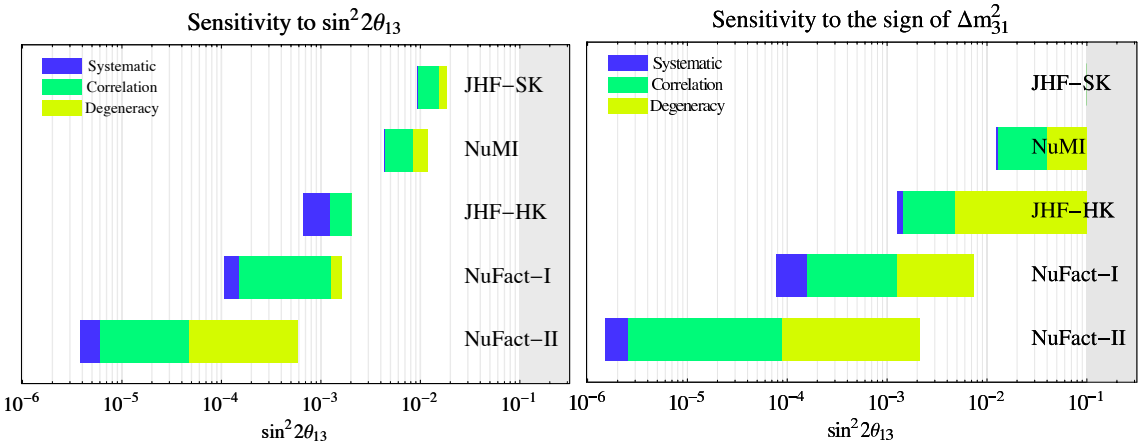

Figure 6: Left plot: The θ_{13} sensitivity of different future accelerator based neutrino oscillation experiments [20]. Right plot: The θ_{13} values for which sensitivity to matter effects, i.e. $sign(\Delta m^2_{31})$ exists. The shown bands are again the reduction of sensitivity from a purely statistical limit (left end of the dark grey/blue range) by systematics (right end of dark grey/blue), correlations (medium grey/green) and degeneracies (light grey/yellow). The right end of the light grey(yellow) band represents the final 90% CL limit. The grey area for large $\sin^2 2\theta_{13}$ indicates the current limit from the CHOOZ experiment.

5. Theoretical implications and conclusions

One of the most interesting unsolved topics is the origin of of flavour and fermion masses. There exist apparent regularities in the fermionic field content which make it very tempting to introduce right-handed neutrino fields leading to both Dirac and Majorana mass terms for neutrinos. Diagonalization of the resulting mass matrices yields Majorana mass eigenstates and due to the see-saw mechanism very small neutrino masses. This can be nicely realized in embeddings of the SM into GUTs with larger symmetries, such as SO(10). Before the discovery of large leptonic mixing, many theorists expected the leptonic mixings to be similar to quark mixing, characterized by small mixing angles. Experiment led theory in showing the striking results that $\sin^2 2\theta_{23} \simeq 1$ and $\tan^2 \theta_{12} \simeq 0.39$, while θ_{13} is small. By finding two large mixing angles, neutrino physics has already provided surprising and very valuable information which severely constrains models of neutrino masses. Future neutrino oscillation experiments will lead to very precise measurements which are also very valuable, since they will provide precision tests of the flavour sector. The level of precision will confirm or rule out many ideas about the origin of flavour and connected topics.

One topic is the small value of $\sin^2 2\theta_{13}$. Since there are two large mixing angles, there is no particular reason to expect the third angle, θ_{13}, to be extremely small or even zero. A small value of $\sin^2 2\theta_{13} \simeq 0.1$ could be a numerical coincidence in a

framework which predicts generically large or sizable mixings. However, if the limit on $\sin^2 2\theta_{13}$ would become smaller by an order of magnitude then some protective mechanism like a "symmetry" would be required. This can be seen in neutrino mass models which are able to predict the large values for θ_{12} and θ_{23}. Such models have a certain tendency to predict a sizable value of θ_{13} as can be seen, for example, in[49,50,51,52,53,54]. The conclusion is that a value of θ_{13} close to the CHOOZ bound would be quite natural, while much smaller values are less likely or hard to understand.

Future precision measurements can also test if relations like $\theta_{23} = \pi/4$ or $\theta_{12}+\theta_C = \pi/4$ which are currently fulfilled within experimental errors still hold at the percent level or below. If so, then this would provide strong constrains on the origin of the flavour structure. Precision is also valuable, even if such special relations are not found. The point is that it is generally not easy to predict a set of very precisely known masses and mixings in a certain model or class of models.

Neutrino masses and mixing parameters are also subject to quantum corrections between low scales, where measurements are performed, and high scales where some theory typically predicts the masses and mixings. This has interesting implications, since it implies that certain deviations from special relations are expected due to quantum corrections (renormalization group or RGE effects). Suppose, for example, that some theory were able to predict $\theta_{13} \equiv 0$. Then RGE effects would still predict a tiny, but finite value at low energy. Strictly speaking, $\theta_{13} = 0$ cannot be excluded completely by this argument, as the high-energy value could be just as large as the change due to running and of opposite sign. However, a complete cancellation of this kind would be a miraculous fine-tuning, since the physics generating the value at high energy is not directly related to quantum corrections at lower energies. The strength of the running of θ_{13} depends on the neutrino mass spectrum and whether or not supersymmetry is realized. For the Minimal Supersymmetric Standard Model one finds a shift $\Delta \sin^2 2\theta_{13} > 0.01$ for a considerable parameter range, i.e. one would expect to measure a finite value of θ_{13} [55]. Conversely, limits on model parameters would be obtained if an experiment were to set an upper bound on $\sin^2 2\theta_{13}$ in the range of 0.01. In any case, it should be clear that a precision of the order of quantum corrections to neutrino masses and mixings is very interesting in a number of ways.

Precision measurements would also allow very interesting tests of many other topics, like MSW matter effects, three neutrino unitarity, neutrino decay, de-coherence and NSI effects. There exists also an interesting interplay with theories beyond the Standard Models, flavour models as well as astroparticle physics (leptogenesis, supernovae, nucleosynthesis, structure formation). In summary, future precision oscillation experiments will provide the best window into the so far un-understood flavour sector. It may give us a glimpse on the origin of flavour, but it may also lead to unexpected results and insights as it happened before in neutrino physics.

Acknowledgments: Work supported by the "Sonderforschungsbereich 375 für Astro-Teilchenphysik der Deutschen Forschungsgemeinschaft".

6. References

1) T. Toshito (SuperKamiokande Collab.), proceedings of 36th Rencontres de Moriond on Electroweak Interactions and Unified Theories, Les Arcs, France, 10-17 Mar 2001, hep-ex/0105023.
2) W. Hampel *et al.* (GALLEX Collab.), Phys. Lett. B **447** (1999) 127.
3) A. B. McDonald (SNO Collab.), proceedings of the Nobel Symposium 129: Neutrino Physics, Haga Slott, Enkoping, Sweden, 19-24 Aug 2004, arXiv:hep-ex/0412060.
4) Q. R. Ahmad *et al.* (SNO Collab.), Phys. Rev. Lett. **89** (2002) 011301, nucl-ex/0204008.
5) A. Suzuki (KamLAND Collab.), Nucl. Phys. Proc. Suppl. **137** (2004) 21.
6) K. Eguchi *et al.* (KamLAND Collab.), Phys. Rev. Lett. **90** (2003) 021802, hep-ex/0212021.
7) E.D. Church, K. Eitel, G.B. Mills and M. Steidl, Phys. Rev. D **66** (2002) 013001, hep-ex/0203023.
8) Y. Suzuki, Nucl. Phys. Proc. Suppl. **137** (2004) 5.
9) M. C. Gonzalez-Garcia, arXiv:hep-ph/0410030.
10) S. Fukuda *et al.*, Phys. Lett. B **539** (2002) 179; B.T. Cleveland *et al.*, Astrophys. J. **496**(1998) 505; D.N. Abdurashitov *et al.*, Phys. Rev. **C60** (1999) 055801; W. Hampel *et al.*, Phys. Lett. **B447** (1999) 127; C. Cattadori, Nucl. Phys. B (Proc. Suppl.) **110** (2002) 311; Q. R. Ahmad *et al.*, Phys. Rev. Lett. **89** (2002) 011301; Phys. Rev. Lett. **89** (2002) 011302.
11) SNO collaboration, submitted to Phys. Rev. Lett. 2003, nucl-ex/0309004.
12) M. Apollonio *et al.*, Phys. Lett. B **420** (1998) 397.
13) M. Apollonio *et al.*, Eur. Phys. J. C **27** (2003) 331.
14) F. Boehm *et al.*, Phys. Rev. Lett. **84** (2000) 3764.
15) M. Maltoni, T. Schwetz, M.A. Tortola and J.W.F. Valle, New Jour. Phys. **6**, (2004) 122, hep-ph/0405172; Phys. Rev. D **68**, (2003) 113010, hep-ph/0309130.
16) M. Freund, P. Huber and M. Lindner, Nucl. Phys. B **585** (2000) 105, hep-ph/0004085.
17) M. Freund, P. Huber and M. Lindner, Nucl. Phys. B **615** (2001) 331, hep-ph/0105071.
18) P. Huber, M. Lindner and W. Winter, Nucl. Phys. B **654** (2003) 3, hep-ph/0211300.
19) M. Lindner, in 'Neutrino mass', Springer tracts in modern physics, ed. by G. Altarelli and K. Winter, hep-ph/0209083.
20) P. Huber, M. Lindner and W. Winter, Nucl. Phys. B **645** (2002) 3, hep-ph/0204352.

21) K. Dick, M. Freund, M. Lindner and A. Romanino, Nucl. Phys. B **562** (1999) 29, hep-ph/9903308.
22) M. Freund, Phys. Rev. **D64** (2001) 053003, hep-ph/0103300.
23) E. K. Akhmedov, R. Johansson, M. Lindner, T. Ohlsson and T. Schwetz, JHEP **0404** (2004) 078, hep-ph/0402175.
24) A. Cervera *et al.*, Nucl. Phys. **B579** (2000) 17, erratum ibid., Nucl. Phys. **B593**, (2001) 731.
25) H. Minakata, H. Sugiyama, O. Yasuda, K. Inoue and F. Suekane, Phys. Rev. D **68** (2003) 033017, hep-ph/0211111.
26) P. Huber, M. Lindner, T. Schwetz and W. Winter, Nucl. Phys. B **665** (2003) 487, hep-ph/0303232.
27) P. Huber and W. Winter, Phys. Rev. D **68** (2003) 037301, hep-ph/0301257.
28) G. L. Fogli and E. Lisi, Phys. Rev. D **54** (1996) 3667, hep-ph/9604415.
29) V. Barger, D. Marfatia, and K. Whisnant, Phys. Rev. **D65** (2002) 073023, hep-ph/0112119.
30) M. Koike, T. Ota and J. Sato, Phys. Rev. D **65** (2002) 053015, hep-ph/0011387.
31) J. Burguet-Castell, M.B. Gavela, J.J. Gomez-Cadenas, P. Hernandez and O. Mena, Nucl. Phys. **B608** (2001) 301, hep-ph/0103258.
32) H. Minakata and H. Nunokawa, JHEP **10** (2001) 001, hep-ph/0108085.
33) J. Burguet-Castell, M.B. Gavela, J.J. Gomez-Cadenas, P. Hernandez and O. Mena, Nucl. Phys. B **646** (2002) 301, hep-ph/0207080.
34) V. Barger, D. Marfatia and K. Whisnant, Phys.Rev. **D66** (2002) 053007, hep-ph/0206038.
35) P. Huber, M. Maltoni and T. Schwetz, hep-ph/0501037.
36) A. Donini, D. Meloni and P. Migliozzi, Nucl.Phys. B **646** (2002) 321, hep-ph/0206034.
37) E. Ables *et al.* (MINOS) FERMILAB-PROPOSAL-P-875.
38) P. Aprili *et al.* (ICARUS) CERN-SPSC-2002-027.
39) D. Duchesneau (OPERA), hep-ex/0209082.
40) Y. Itow *et al.*, hep-ex/0106019.
41) D. Ayres *et al.*, hep-ex/0210005,
42) K. Anderson *et al.*, hep-ex/0402041.
43) F. Ardellier *et al.*, hep-ex/0405032.
44) P. Huber, M. Lindner, M. Rolinec, T. Schwetz and W. Winter, Phys. Rev. D **70** (2004) 073014, hep-ph/0403068.
45) P. Huber, M. Lindner and W. Winter, GLoBES (Global Long Baseline Experiment Simulator), hep-ph/0407333, to appear in Comp. Phys. Comm., http://www.ph.tum.de/~globes.
46) H. Minakata, M. Sonoyama and H. Sugiyama, Phys. Rev. D **70** (2004) 113012, hep-ph/0406073.

47) P. Huber, M. Lindner, M. Rolinec, T. Schwetz and W. Winter, hep-ph/0412133.
48) P. Huber, M. Lindner, T. Schwetz and W. Winter, Nucl. Phys. B **665** (2003) 487, hep-ph/0303232;
49) S. M. Barr and I. Dorsner, Nucl. Phys. B **585** (2000) 79, hep-ph/0003058.
50) G. Altarelli and F. Feruglio, in 'Neutrino Mass', Springer Tracts in Modern Physics, ed. by G. Altarelli and K. Winter, hep-ph/0206077.
51) R. Barbieri, T. Hambye and A. Romanino, JHEP **0303** (2003) 017, hep-ph/0302118.
52) M. C. Chen and K. T. Mahanthappa, Int.J.Mod.Phys. **A18** (2003) 5819, hep-ph/0305088.
53) S. F. King, Rept. Prog. Phys. **67** (2004) 107, hep-ph/0310204.
54) H. S. Goh, R. N. Mohapatra and S. P. Ng, Phys. Rev. D **68** (2003) 115008, hep-ph/0308197.
55) S. Antusch, J. Kersten, M. Lindner and M. Ratz, Nucl. Phys. B **674** (2003) 401, hep-ph/0305273.